nature biomedical engineering

SUPPLEMENTARY INFORMATION

DOI: 10.1038/s41551-017-0142-5

In the format provided by the authors and unedited.

A growth-accommodating implant for paediatric applications

Eric N. Feins[1], Yuhan Lee[2], Eoin D. O'Cearbhaill[2,4], Nikolay V. Vasilyev[1], Shogo Shimada[1], Ingeborg Friehs[1], Douglas Perrin[1], Peter E. Hammer[1], Haruo Yamauchi[1], Gerald Marx[3], Andrew Gosline[1], Veaceslav Arabagi[1], Jeffrey M. Karp[2]* and Pedro J. del Nido[1]*

[1]Department of Cardiac Surgery, Boston Children's Hospital, Harvard Medical School, 300 Longwood Avenue, Boston, MA 02115, USA. [2]Engineering in Medicine Division, Department of Medicine, Center for Regenerative Therapeutics, Brigham and Women's Hospital, Harvard Medical School, Harvard Stem Cell Institute, Harvard-MIT Division of Health Sciences and Technology, 60 Fenwood Road, Boston, MA 02115, USA. [3]Department of Cardiology, Boston Children's Hospital, Harvard Medical School, 300 Longwood Avenue, Boston, MA 02115, USA. Present address: [4]School of Mechanical and Materials Engineering, University College Dublin Centre for Biomedical Engineering, and University College Dublin Conway Institute of Biomolecular and Biomedical Research, University College Dublin, Belfield, Dublin 4, Ireland. Eric N. Feins and Yuhan Lee contributed equally to this work.
*e-mail: bwhkarp@gmail.com; pedro.delnido@cardio.chboston.org

Contents

1. Supplementary Materials and Methods

1.1. Ex vivo 1-dimensional testing. A biaxial nitinol braided sleeve (Creganna Medical) and a hard sugar spherical core served as the rudimentary device prototype. The braided sleeve was tied down on either side of the spherical core using poly(ethylene terephthalate) suture (Ethibond Excel®, Ethicon). The braid/core was suspended above the water level in a water tank, and a 2 N tensile force was applied to the braided sleeve using a pulley system. At time point "zero" the braid/core was lowered into the water and the sleeve length and diameter were measured. Sleeve length was defined as the distance between the two Ethibond® sutures. Sleeve diameter was measured with calipers at the center of the spherical core. Length and diameter measurements were obtained at 5-minute intervals until the entire sugar core had dissolved. Mean braided sleeve length and diameter at each time point were calculated from the data (n = 4) and plotted against time to characterize the braided sleeve elongation and thinning profiles.

1.2. Ex vivo 2-dimensional testing. An ethylene chlorotrifluorethylene (ECTFE) biaxially braided sleeve (McMaster-Carr®) and heat-molded hard sugar spheres were used for the device prototype. Sugar spheres were molded to a diameter of 6.3 mm. After cooling and hardening, the spheres were inserted into the braided sleeve. The braided sleeve ends were then sealed by melting the braid fibers together under an open flame.

The isolated swine heart preparation involved a freshly explanted swine heart placed in a water tank after removal of the right atrium to expose the tricuspid valve. The pulmonic valve was cut, and the main pulmonary artery was cannulated and attached to a water column (Supplementary Fig. S1a). This enabled pressurizing of the right ventricle to physiologic levels (20-30 mmHg). An *en face* image of the valve was obtained for post-hoc valve area measurement. The ring was then sutured to the valve annulus using Ethibond Excel® sutures, which reduced the valve size by approximately 25% (Supplementary Fig. S1b,c). Once implanted, the heart was placed underwater to enable sugar core dissolution and braided sleeve elongation (Supplementary Fig. S1d). Pressurizing the right ventricle exposed the device to radial and tensile forces, which helped drive sleeve elongation in the setting of core dissolution. *En face* images of the tricuspid valve and ring were obtained immediately after submerging in water, and then at 2-minute intervals until the sugar cores had completely dissolved and the braided sleeve had completely elongated. Valve areas were calculated by analyzing the *en face* valve images with MATLAB software (MathWorks®).

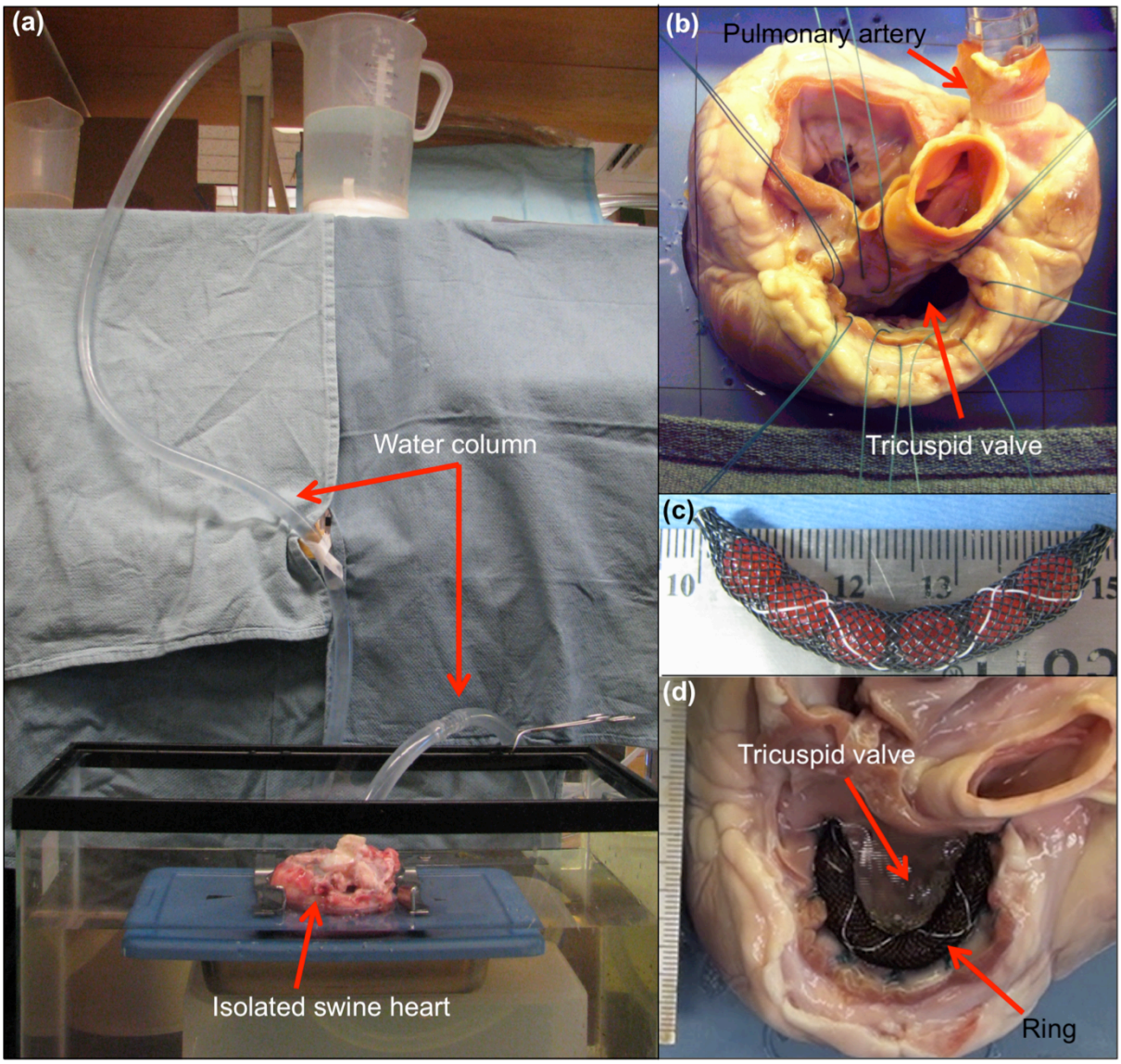

Figure S1 | Images of experimental set-up for *ex vivo* 2-D growth testing in isolated swine heart preparation. **a**, Overall set-up with explanted swine heart placed in water tank. Pulmonary artery is cannulated with tubing that contains water column. Unclamping of tubing enables physiologic pressurization of heart by water column. **b**, *En face* view of tricuspid valve after removal of right atrium. Sutures have been placed around tricuspid valve annulus, which are used to implant the growth-accommodating ring. **c**, Growth-accommodating ring prototype composed of ECTFE biaxially braided sleeve (black) and inner spherical sugar cores (red). **d**, *En face* view of tricuspid valve after implantation of ring onto valve annulus.

1.3. Linear tensile and cyclic fatigue tensile tests using mechanical tester. Mechanical testing was performed on an ADMET eXpert 7601 universal tester, equipped with a 50 N load cell and using the device with a cylindrical extra-stiff poly(glycerol sebacate) ESPGS core (length: 10 mm, diameter: 1.8 mm) and an outer ultra-high-molecular-weight polyethylene (UHMWPE) braided sleeve. The device was mounted on the tester by each end of the braid, such that tensile stress on the braid would cause compressive stress on the polymer core. Uniaxial tensile testing was performed at a jog rate of 10 mm/min until sample failure ($n > 3$ per condition), and Young's modulus was calculated as the slope at 20% strain. ESPGS cores cured for 24, 42, 62,

or 86 hours were compared to evaluate the effect of polymer core mechanical strength on the overall tensile strength of the device. Cyclic fatigue tensile testing (n = 3) was performed at a jog rate of 50 mm/min, by sample extension until 30% elongation during 1000 consecutive cycles. Stress-strain curves were recorded every 100 cycles.

1.4. In vitro testing of core degradation in relation to mechanical properties of device.

The relationship between core degradation rate and tensile stress was studied to assess whether degradation was significantly affected by the external stresses of growing tissue. Devices composed of a cylindrical ESPGS core (diameter: 1.8 mm) and an outer UHMWPE braided sleeve were mounted in a 0.1 M NaOH solution to produce accelerated degradation conditions, and a weight was applied to produce a defined tensile stress (buoyancy adjusted) for a 12-day period (Fig. S2a). Core erosion was assessed by measuring core diameter at 0, 1, 2, 4, 7 and 12 days using an electronic digital caliper (n = 3 in each arm). At day 7 after degradation in 0.1M NaOH solution (average 44.6% reduction in diameter), tensile strengths of the devices were measured using the universal mechanical tester (n = 3) (Fig. S2b). The tensile testing was performed at a jog rate of 8 mm/min until it reached the force sensor limit (50N). The mechanical profiles of devices with non-degraded and partially degraded cores were similar, suggesting that device strength would be well preserved throughout the core degradation process following implantation (Fig. S2c).

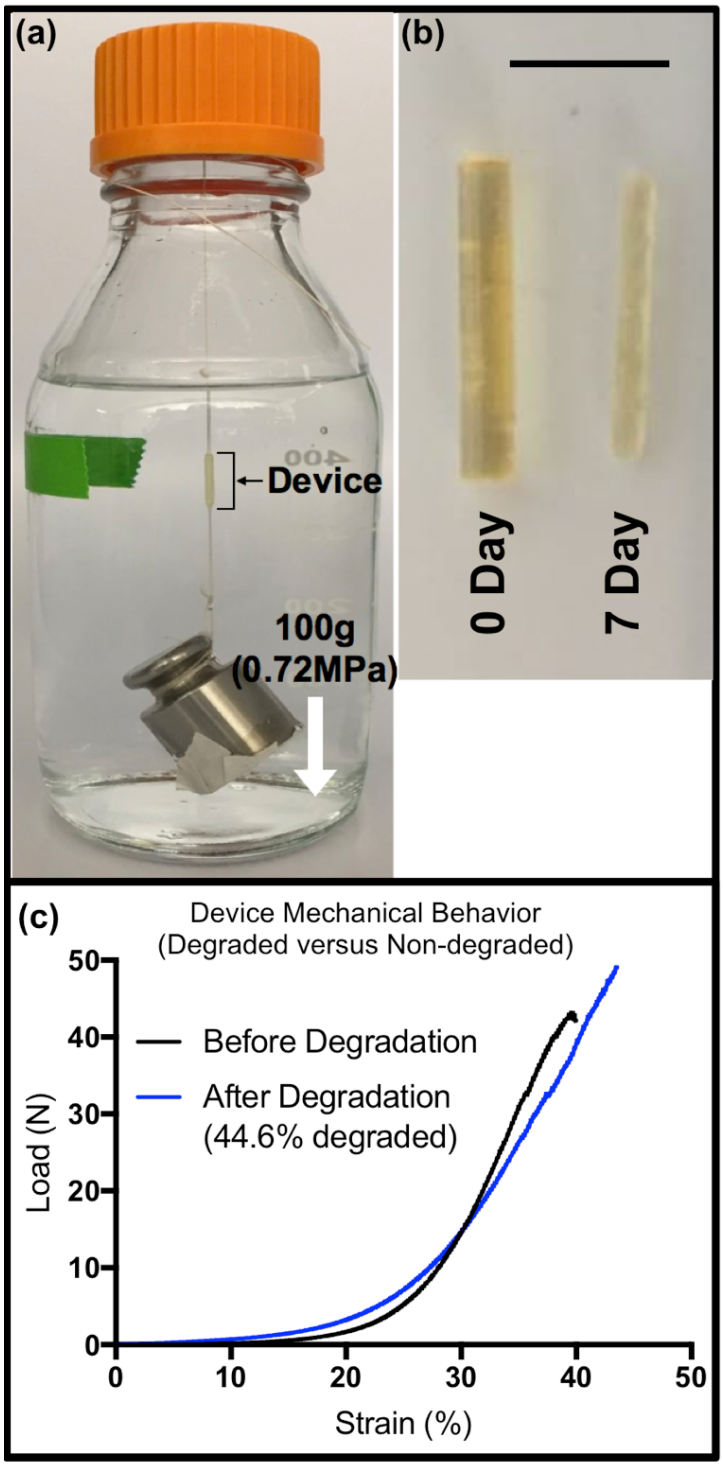

Figure S2 | Ex vivo testing of core degradation in relation to mechanical properties of device. a, Experimental setup for testing effect of tensile load on polymer core degradation. Device is suspended in 0.1M NaOH solution with defined tensile load. **b**, Representative ESPGS cores at day 0 (left) and day 7 (right) (scale bar = 5 mm). **c**, Comparison of mechanical profile of device with non-degraded core (−) versus device with partially degraded core (−). Mechanical profile is similar despite partial core degradation.

1.5. In vivo bone growth model. Growing male Wistar rats (150-200 g, Charles River Laboratories International) were used for the study. Anesthesia was initiated with ketamine and xylazine (intra-peritoneal) and inhaled isoflurane, and then maintained with isoflurane. After endotracheal intubation and initiation of ventilation the left hind leg was shaved and disinfected with topical povidone-iodine solution. An incision was made along the left tibia and dissection was carried out down to the bone. After identification of the growth plate, a hole was drilled through the proximal epiphysis and the distal diaphysis beyond the insertion of the fibula. The device was then sutured through the holes to the tibia using the polypropylene anchoring sutures on the device. The anchoring sutures were tied down tightly to eliminate as much slack as possible in the device. Bupivacaine 0.25% was then injected in the incision and the skin was closed with a Chromic Gut suture (Ethicon). Prior to awakening from anesthesia, the animals underwent post-operative imaging of their bilateral tibias using a MicroCAT II CT scanner (Siemens). Interval CT imaging was performed to assess bilateral tibial length. During these post-operative studies the animals were placed under anesthesia with 1.5-3.0% inhaled isoflurane. At the completion of the study all rats were euthanized with carbon dioxide, and the hind legs were explanted. Four animals received a growth-accommodating device with a degradable ESPGS core. One of these animals was excluded from the analysis due to development of a wound infection, which could have significantly impacted bone growth. Three animals received a fixed-size device with a non-degradable polytetrafluoroethylene (PTFE) core.

Tibial length was measured offline using Amide software (SourceForge) to analyze the micro-CT datasets. Mean tibial length was calculated by averaging all tibial lengths in each group (left ESPGS tibia, left PTFE tibia, right tibia). Polymer diameter in representative animals was also measured with Amide software by using fiducial markers on CT images. To best assess device length in representative animals, plain X-rays of the left tibia were obtained. Radio-opaque markers placed on the ends of the device enabled device length measurement from X-ray images. (Supplementary Fig. S3)

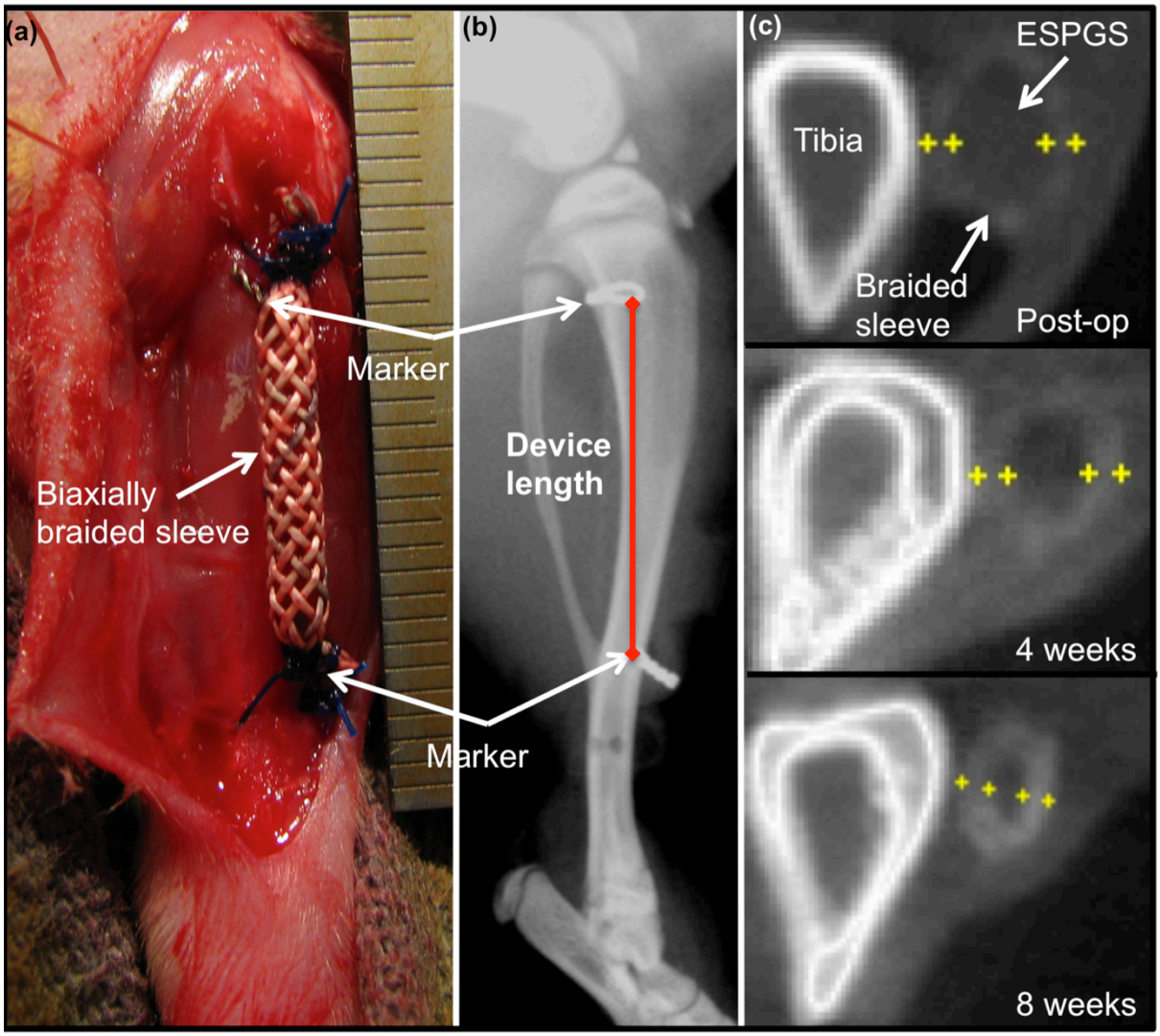

Figure S3 | *In vivo* rat tibial implant setup and imaging. a, Image of growth-accommodating implant immediately after implantation along left tibia prior to skin closure. **b**, X-ray of left tibia & implant post-operatively. Radio-opaque markers at ends of implant allow for measurement of device length (red). **c,** Cross-sectional micro-CT images of left tibia (left) and device implant (right). *Top:* Post-op – immediately following device implantation. *Middle:* 4 weeks after surgery. *Bottom:* 8 weeks after surgery. Fiducial markers (**+**) were used to measure inner polymer diameter over time to assess for ESPGS degradation. Using the ESPGS degradation profile and the mathematical biaxial braid model (equation (1)) the overall device elongation profile was predicted.

1.6. Proof-of-principle heart valve growth model. Female Yorkshire piglets (mean age 7.3 ± 0.9 weeks, mean weight 14.3 ± 1.9 kg, Parsons EM & Sons Inc.) were anesthetized using intramuscular (IM) injection of telazol (4.4 mg/kg), xylazine (2.2 mg/kg), and atropine (0.04 mg/kg), and then intubated with a cuffed endotracheal tube and ventilated with a volume-control ventilator (Fabius Tiro; Draeger Medical, Andover, MA). Anesthesia was maintained with inhaled desflurane (4-9%). A transurethral urinary catheter was inserted for monitoring of urine output. Arterial and central venous lines were placed percutaneously in the femoral artery and vein for arterial and central venous pressure monitoring, respectively. Electrocardiogram and temperature monitoring were accomplished via esophageal and rectal probes, respectively. The chest and groin were disinfected with povidone-iodine and alcohol solutions. Access to the heart

and tricuspid valve was obtained by performing a right thoracotomy or a median sternotomy. We changed from thoracotomy to sternotomy midway through the study because sternotomy provided better exposure of the tricuspid valve with less manipulation of the right lung. Baseline 2-D and 3-D echocardiography were performed using a matrix array ultrasound probe X7-2 (2-7 MHz) on an iE33 system (Philips Healthcare) to assess tricuspid valve size and overall heart function. After intravenous heparin administration (300 U/kg) to achieve an activated clotting time of >350 seconds, arterial cannulation was performed via the femoral artery. Bicaval venous cannulation was performed, and cardiopulmonary bypass was initiated using an oxygenator (FX25, Terumo Medical Corporation). Fentanyl (50-200 μg/kg) and midazolam (0.2 mg/kg) were administered for anesthesia during cardiopulmonary bypass. With the animal cooled to 33°C and under beating-heart conditions, the right atrial appendage was opened to expose the tricuspid valve. The valve was then sized using custom-made sizers, which were designed using SolidWorks software and manufactured out of acrylic. Sizer geometry was based on commercially available tricuspid ring sizers (Edwards) (Supplementary Fig. S4a). The valve sizers were downsized to accommodate piglet heart valves (Supplementary Fig. S4b). Ring prototypes were mounted on a custom-made mounting device to facilitate implantation (Supplementary Fig. S4c,d,e). Intra-operatively the valve was sized by measuring the length of the septal leaflet at the time of surgery – a conventional surgical technique – and was then reduced by one ring size (Table S1). Implantation involved suturing the body and ends of the ring to the annular tissue with Ethibond® sutures (Ethicon). After implanting the ring, the right atrial appendage was closed and hemostasis was obtained. Animals were weaned off cardiopulmonary bypass and arterial and venous cannulas were removed. 2-D and 3-D echocardiography were performed to establish baseline post-operative valve size. Color and continuous wave Doppler echocardiography were performed to assess valve function. The chest and groin incisions were then closed, and two chest tubes were left in place for drainage. The animals were recovered in the OR, with removal of all monitoring lines and chest tubes prior to awakening from anesthesia. After awakening from anesthesia the endotracheal tube was removed and the animals were brought to the pen for further recovery.

Interval transthoracic echocardiography was performed every 2 weeks to assess heart function and ring position. During this procedure the animals were kept under deep sedation with telazol 4.5 mg/kg IM, xylazine 2 mg/kg IM, atropine 0.04 mg/kg IM, and inhaled isoflurane 1-3%. At the time of euthanasia, animals were placed under anesthesia using the aforementioned regimen. Median sternotomy was performed, and the heart was exposed. 2-D and 3-D epicardial echocardiography were performed to assess tricuspid valve size. Color and continuous wave Doppler echocardiography were used to assess valve function. The animals were then euthanized by intravenous injection of overdosed pentobarbital sodium (Fatal-Plus®, 86 mg/kg). The heart was then excised and opened for direct inspection.

Tricuspid valve size (i.e. cross-sectional area of the annulus) was measured offline by analyzing full-volume echocardiography datasets using the multi-planar 3D quantification mode of the QLAB software (Philips Healthcare). Valve area was then plotted to assess valve area reduction by the annuloplasty ring at the time of implantation, and subsequent valve growth. Tricuspid valve function (i.e. valve stenosis/regurgitation) was evaluated offline by assessing for turbulent transvalvular blood flow on 2-D color Doppler echocardiography which would indicate valve stenosis, and by assessing for regurgitant blood flow. Additionally, transvalvular gradients were measured with continuous wave Doppler echocardiography (Fig 4j).

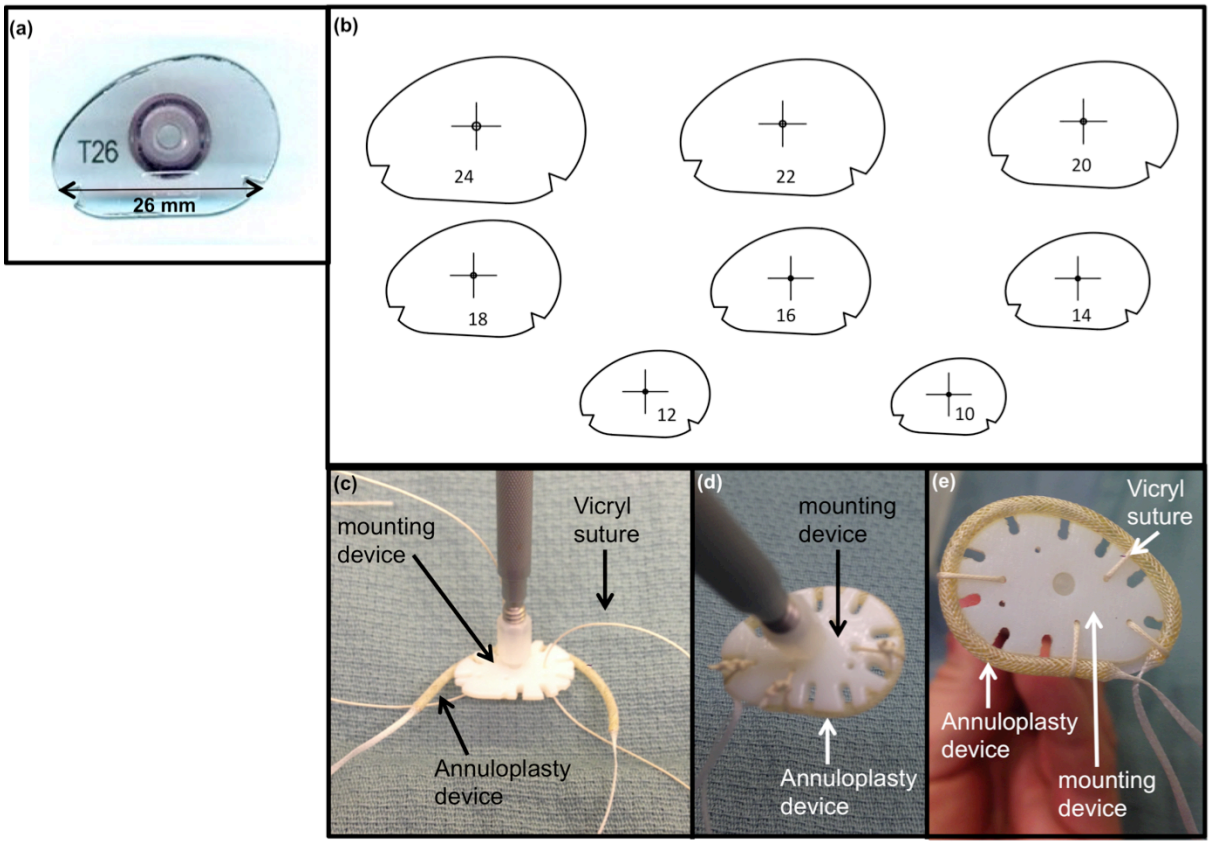

Figure S4 | Growth-accommodating annuloplasty ring design and production. a, Image of Edwards tricuspid ring sizer (size 26 mm), which formed the basis for ring sizers in the swine study. **b,** Downsized ring sizers designed using SolidWorks for use on piglet heart valves. **c,** Braid/polymer prototype – fixing ring to mounting device facilitated surgical implantation. **d,** Top view of growth-accomodating implant fixed to mounting device. The mounting device – composed of acrylic – has notches to allow for passage of sutures around ring during surgical implantation. **e,** Undersurface of mounting device with growth-accomodating implant fixed around it.

Animal	Age (wk)	Weight (kg)	Valve size/Ring size (mm)
1	8.6	16.9	24/22
2	6.9	14.3	24/22
3	6.9	13.4	22/20
4	6.9	12.4	20/18

Table S1 | Animal Summary of Piglet Heart Model

2. Supplementary Video

Video S1

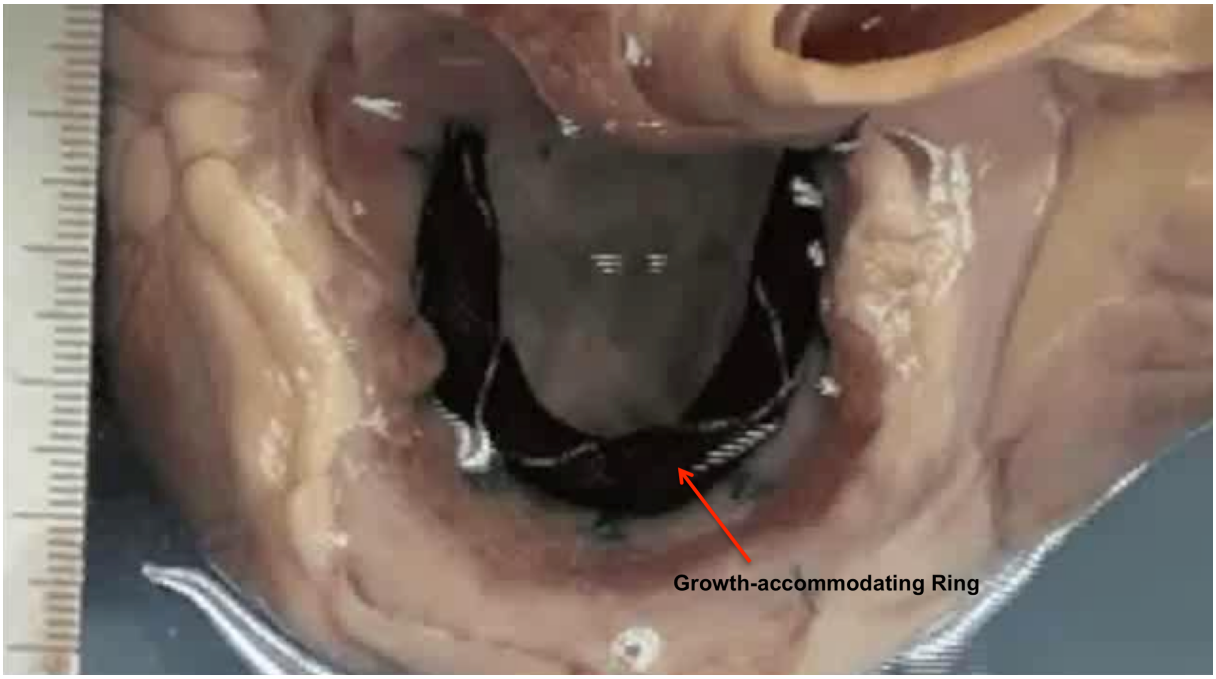

Video S1 | Representative video of growth-accommodating annuloplasty ring in *ex vivo* swine heart preparation. Video is *en face* view of tricuspid valve with ring in place. 100x normal speed demonstrates gradual ring and tricuspid valve expansion in response to inner core dissolution.